Journal of the Korean Vacuum Society
Vol. 8, No. 3(2), August 1999, pp. 327~332

Growth studies of chromium thin films using real-time spectroscopic ellipsometry

Yongdal Lee, Jiyong Jung, Kyoungyoon Bang, Hyegeun Oh and Ilsin An

Department of Physics and Center for Electronic Materials and Components, Hanyang University, Ansan, 425-791 Korea
(Received February 24, 1999)

실시간 분광 엘립소미트리를 이용한 크롬 박막의 성장 연구

이용달 · 정지용 · 방경윤 · 오혜근 · 안일신

한양대학교 물리학과 및 전자재료 및 부품센터
(1999년 2월 24일 접수)

Abstact – High speed real-time spectroscopic ellipsometry was employed in order to characterize the growth of chromium thin film. This instrument can collect 512 points of {Δ(hv), Ψ(hv)} spectra from 1.3 to 4.5 eV with acquisition and repetition rates of 20 msec or less. When this instrument was integrated into the chromium thin film growth, we could obtain not only the information on film properties but also the details of the processes. We deduced the growth rates and the evolution of the optical properties of chromium thin films under several preparation conditions. We also demonstrated the contamination process of chromium thin films caused by air exposure.

요 약 – 고속 실시간 분과 엘립소미트리를 이용하여 크롬 박막의 성장을 연구하였다. 이 장비는 1.3 eV에서 4.5 eV에 걸쳐 512개의 {Δ(hv), Ψ(hv)}를 가진 스펙트럼을 20 msec 이하의 속도로 연속하여 측정할 수 있는데, 크롬 박막 성장에 적용하였을 때 박막의 성질뿐만 아니라 공정과정에 관련된 정보까지 얻을 수 있었다. 각기 다른 증착조건에서 증착률 및 광학적 특성의 시간적 변화를 구할 수 있었으며 공정에서 대기 노출로 인한 오염과정을 보여줄 수 있었다.

I. Introduction

Determination of material properties in real time during preparation or processing is an important issue in materials research. Many technologically important materials are in the form of thin films and they are prepared in adverse environments such as chemical solutions, plasmas, and vacuum, etc. In these situations, ellipsometry is among the few non-invasive techniques of real-time characterization. As ellipsometry analyzes the states of polarization upon reflection from specular surface, it has monolayer sensitivity through the detection of phase change. With the development of real-time single wavelength ellipsometers for fast data acquisition, ellipsometry has been employed to characterize thin films during the growth and modification. However, the information deduced from the single wavelength was limited to the studies of growth pattern [1]. Recently, fast scanning spectroscopic ellipsometry has been developed using multichannel detector. This instrument has been used for the real-time characterization of thin film growth and surface modification both in electrochemical and vacuum processes [2-6].

Since the first version of this instrument was introduced, much improvement has been achieved in precision as well as in data acquisition speed [7-9]. In this work, we developed our own real-time spectroscopic ellipsometer (RTSE) equipped with multichannel detection system. The acquisition and repetition rates for ellipsometric spectra be-

came at least five times higher than those of the previously reported one [9]. This instrument was integrated into the sputtering system in order to monitor the growth of chromium (Cr) thin films.

Cr is the base material for the optical mask in semiconductor lithography. As the wavelength of the optical lithography becomes shorter for better resolution, a new material is needed to meet the optical requirements at shorter wavelength. In this work, we varied the deposition conditions for the possible modification of the optical properties of Cr films. This can be achieved by introducing void into the film or controlling the size of metal grains. Cr thin film is also used as an adhesion layer to deposit other metallic thin films on it. Thus, it is very important to understand the growth mechanism of Cr thin film.

The goal of this work is to demonstrate the ability of the RTSE in the fields where the real-time characterizations are needed. Thus, we show the growth processes of Cr films under different deposition conditions. Also we show the contamination processes during and after deposition.

II. Experimental

Fig. 1 shows the configuration of RTSE and turbo-pumped sputtering system used in the experiment. The RTSE was designed in the rotating polarizer configuration. It consists of 75 W Xe-source, polarizer with rotational frequency of 15-50 Hz, sample in vacuum chamber, analyzer with stepping accuracy of 0.01 degree, grating spectrograph, and 512 channel detection system. Strain-free fused silica ports were developed and mounted on the vacuum chamber for optical access. Instead of using a commercial optical multichannel analyzer, we developed our own multichannel detection system using photodiode array and data acquisition electronics [10]. With this system, we have full access to various data acquisition modes and we can collect 512 spectral points of {Δ, Ψ} over 1.3 to 4.5 eV possibly in less than 20 msec with partial integration method. The detailed information on the operation of similar instrument was reported elsewhere [7-9, 11].

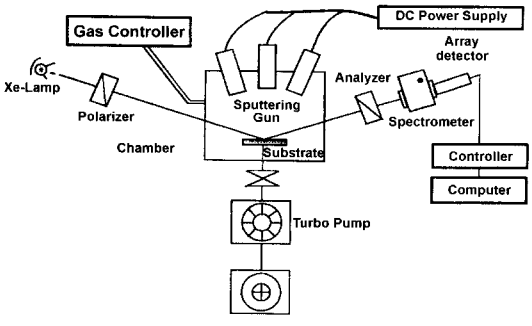

Fig. 1. Real-time spectroscopic ellipsometer and sputtering system used in growth studies.

An rf-magnetron sputtering technique was employed to prepare Cr thin films and the deposition condition was varied in order to control the properties of the films. 10 sccm of pure argon was used as a sputtering gas and crystalline silicon (c-Si) wafer was used as substrate. DC power and argon pressure were varied in this study. After 5 mins of pre-sputtering, each pair of ellipsometric spectra were collected in every second, because the growth rate was low with sputtering.

III. Results and Discussion

Fig. 2 shows the 200s evolution of ellipsometry angle at 3.51 eV during the growth of Cr at three

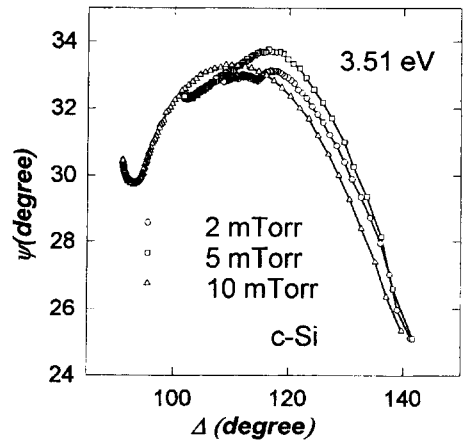

Fig. 2. Optical trajectories obtained during sputtering with different argon pressures. Each point at 3.51 eV was selected from 200 pairs of {Δ, Ψ} spectra over 1.5 and 4.5 eV.

different argon pressures. These trajectories were selected from the 512 spectral points of each {Δ, Ψ} spectra for clear view. Ellipsometry angles {Δ, Ψ} are defined by the ratio of reflectance coefficients, r_p and r_s, where p and s denote the parallel and perpendicular directions of polarization.

$$\tan\Psi e^{i\Delta} = \frac{r_p}{r_s} \quad (1)$$

The common start-points in Figure 2 indicate the optical properties of c-Si substrate and the time interval between two neighboring points is 1 s. We can notice that three trajectories deviate from each other from the beginning of the growth. Near the end of 200 s, the intervals are very close, meaning that the film is almost opaque at 3.51 eV. As the trajectories are different all the way from the beginning to the end, it can be said that these three materials have different optical properties or microstructures.

Fig. 3 shows the dielectric functions of those three Cr thin films (symbols), where $\varepsilon_{1(2)}$ is the real (imaginary) part of the complex dielectric function. The last {Δ, Ψ} spectra in Fig. 2 were directly converted to dielectric function assuming bulk materials. When these dielectric functions are compared to that of well-grown Cr film under optimum condition, clear trend can be seen with increase of argon pressure. The optimum condition in our system is to maintain the target-to-substrate distance below 10 cm at 2 mTorr of working pressure. For ellipsometric measurement, the position of substrate is limited by the optical path. The solid lines show the dielectric function of well-grown Cr and broken or dotted lines show those of low density Cr's calculated from the Bruggeman effective medi-

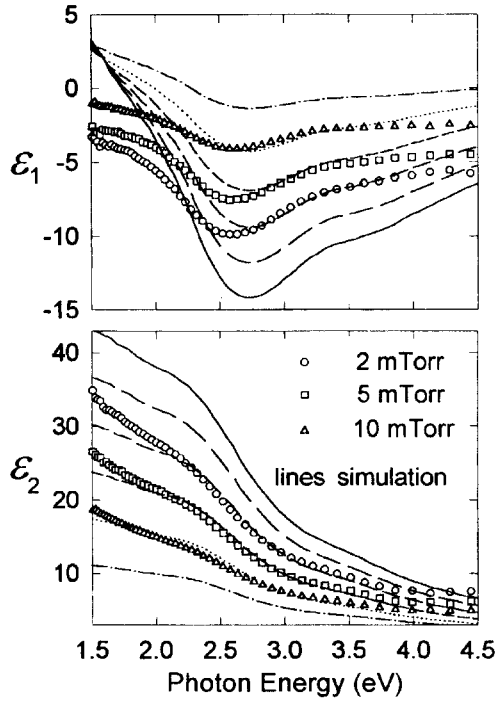

Fig. 3. The dielectric functions after 200 s into deposition with different argon pressures (symbols). These correspond to the end points in Fig. 2. Lines are calculated from the dielectric function of well-grown chromium with assumed void fractions. Solid lines are the dielectric function of well-grown chromium. Following lines show the dielectric functions containing void from 10 to 50% (long dashed lines : 10%, medium dashed lines : 20%, short dashed line : 30%, dotted lines : 40%, dashed lines with dots : 50%).

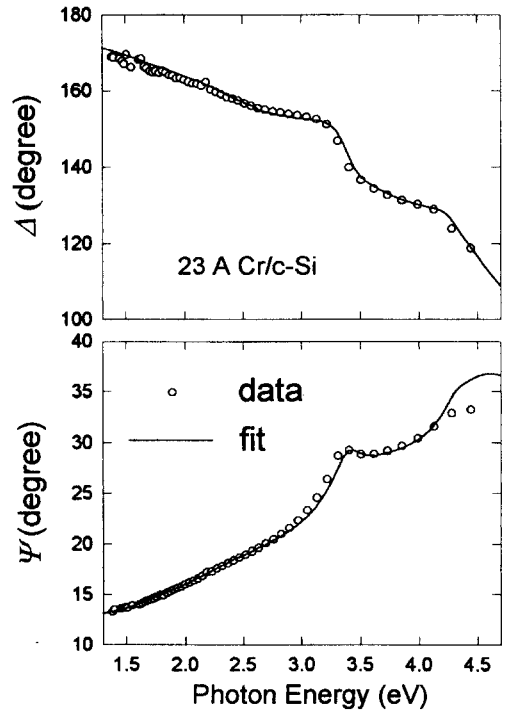

Fig. 4. The spectroscopic fit using the dielectric function of bulk chromium as a reference. Circles: data, Lines: best fit with 1-layer optical model.

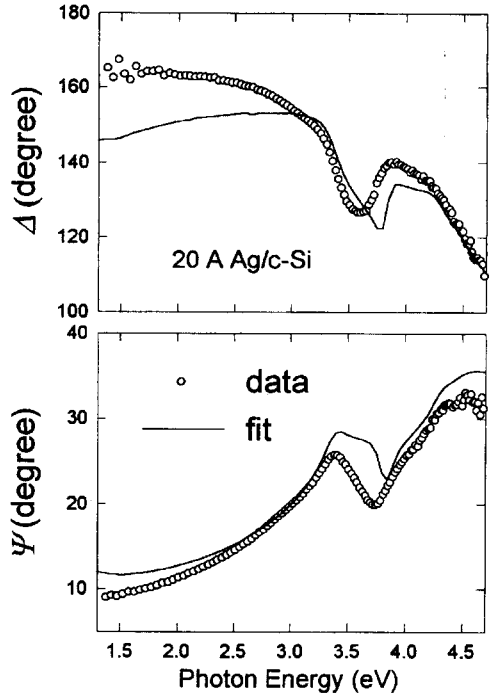

Fig. 5. The spectroscopic fit using the dielectric function of bulk silver as a reference. Circles: data, Lines: best fit with 1-layer optical model.

um theory varying void contents from 10 to 50% [12]. The dielectric function of the low density medium (<ε>) can be obtained from the mixture of well-grown Cr (ε_a) and void (ε_b) in the following equation, where f is the volume fraction of Cr,

$$0 = f\frac{\varepsilon_a - <\varepsilon>}{\varepsilon_a + 2<\varepsilon>} + (1-f)\frac{\varepsilon_b - <\varepsilon>}{\varepsilon_b + 2<\varepsilon>} \qquad (2)$$

The effective dielectric functions above 3.0 eV show the free electron behavior and well explain the quality of Cr films prepared at different sputtering conditions. As the argon pressure increased, the mean free paths of sputtered atoms decreased through the collision process. Thus, the adatoms on the c-Si substrate have less energies when they suffer more collisions. This resulted in the lack of density in the film. Our films in Figure 3 show density deficits ranging from 20 to 40%. Very similar results were reported in the growth of amorphous silicon thin films [4].

When each set of the spectra were analyzed

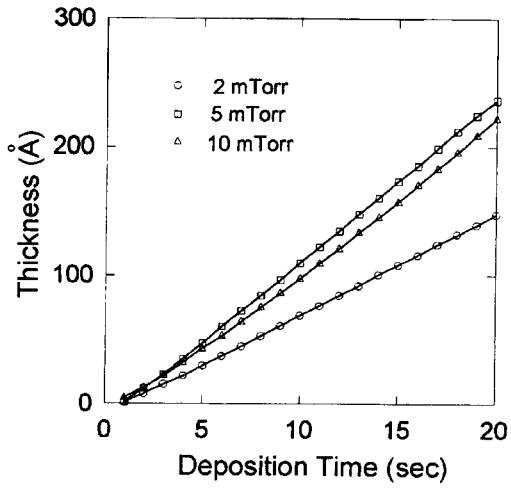

Fig. 6. Variation of thickness deduced from a single-layer optical model.

using the optical simulation, more informations were deduced. However, when we use optical calculations for metal films, we need to be cautious of the size effect. When small grains are formed in the nucleation stage of growth, some metals show strong size-dependant optical properties. In such cases each spectrum should be analyzed independently instead of using reference dielectric function of bulk material [13, 14]. Fig. 4 shows the quality of fit in the optical simulation of ~20Å Cr thin film using the dielectric function of bulk Cr. Although small deviation is noticed at low energy region, overall quality of fit is acceptable. Meanwhile, when we did same analysis for silver thin film, dramatic difference was noticed as shown in Fig. 5. This is due to the size effect caused by the electron scattering at the grain surface [13, 14]. In our future study, we will investigate the growth of Cr in the range of <20 Å to see any possible size effect.

As Cr did not show any significant size effect, we performed optical analysis using bulk dielectric function of Cr to see the growth behavior. In Fig. 6, we find that the growth rate increased as we changed argon pressure from 2 to 5 mTorr. This means that the sputtering yield was lower at 2 mTorr due to the lack of working gas molecules. However, when the pressure was increased again

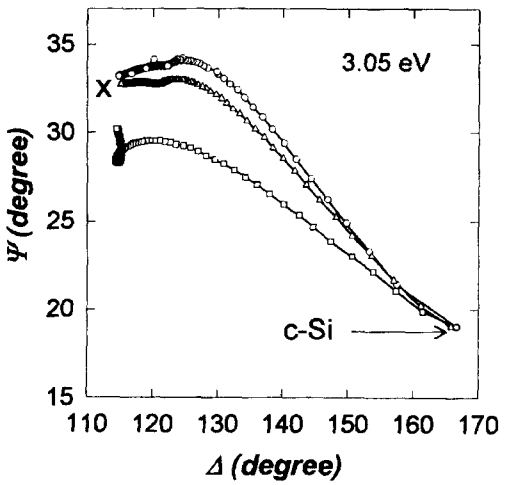

Fig. 7. Optical trajectories obtained during the deposition of chromium under identical deposition conditions except the periods for air exposure of the system and pumping. Circles: 30 s exposure and 3 h pumping, Squares: 30 min exposure and 10 min pumping, Triangles: 30 s exposure and 1 h pumping.

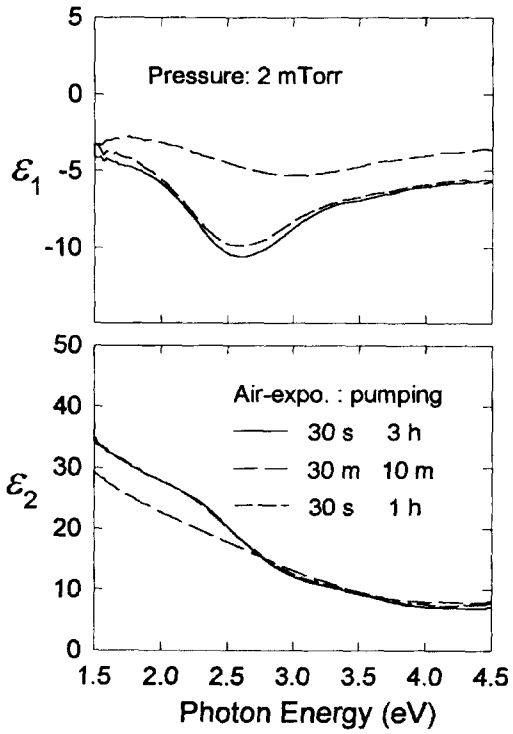

Fig. 8. The dielectric functions deduced from the last points in Fig. 7.

from 5 to 10 mTorr, the growth rate was rather decreased slightly. Although the sputtering efficiency might be increased, we think apparently the scattering process became more dominant at higher pressure. Similar results were obtained from the variation of DC power (not shown)-monotonic increase in growth rate with power and small variations in the optical properties.

Now we want to present the contamination processes of Cr by air exposure. For this experiment we attempted two different approaches. One was using poor pumping process after chamber was exposed to air and the other was venting with air after the end of fresh deposition of Cr film. In vacuum process, it is very important to evacuate chamber sufficiently. This can be ensured by using high vacuum pumping and monitoring the base pressure of the system. In general, pumping should be continued for many hours, because, once exposed to air, the water molecules desorb continuously from the inner surface of chamber. Fig. 7 shows three optical trajectories obtained from the consecutive depositions of Cr films under identical deposition conditions except the pumping process. In the first deposition, the c-Si substrate was mounted quickly to minimize the air exposure of the system and more than three hours of pumping process was followed (circles). In the second deposition, the chamber was opened in air quite a while and a brief pumping was carried out (squares). These two trajectories are quite different. In order to verify the water contamination caused by poor pumping in the second deposition, we repeated the first process with a little less pumping period (three hours vs one hour). Without any analysis, it was quite obvious that the third attempt almost recovered the first process (triangles). This verified that the water vapor on the chamber wall was the main contaminant in the second process. As deposition progresses, the water vapors inside chamber are incorporated into the film or pumped away. Thus, the quality of the film should become better and better as deposition progresses. Interestingly, this phenomenon can be seen at the end of the second trajectory. As the ellipsometry beam sees mostly the upper part of the film within

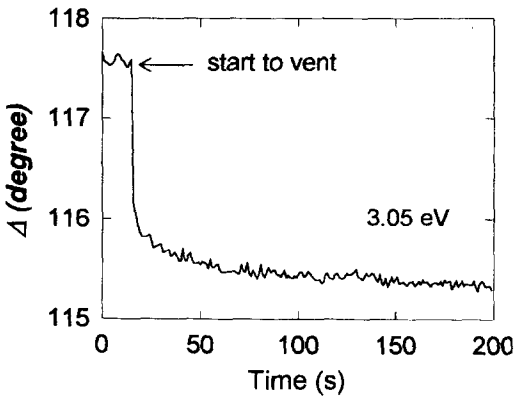

Fig. 9. Ellipsometry angle Δ versus time collected during the 200 s of air introduction after the fresh deposition of chromium.

the optical penetration depth, the second trajectory turns toward the final optical constant of better films as we expected (see mark 'x'). Meanwhile the third trajectory was approaching the first one very closely indicating the fast recovery from less contamination. These results are clearer in Fig. 8, which shows the dielectric functions of these three films deduced from the end points in Fig. 7. The quality of the films can be imagined when we compare with those in Fig. 3. However, the difference in optical properties in this case is caused mainly by the incorporation of chromium oxide rather than void.

The final result shows the magnitude of contamination after the end of deposition. After Cr thin film was deposited, we vented the vacuum system with air very slowly over 150 s. Fig. 9 shows Δ versus time measured during the venting process. This was the oxidation process which we did not observe when gold film was used. Rough estimation with optical analysis showed that a couple of monolayer was formed in less than 20 s.

IV. Summary

We demonstrated the real-time and in situ capabilities of our spectroscopic ellipsometer in chromium thin film growth. Chromium thin films did not show any seizable size effect in the early growth stage (~20 Å). However, the properties of final films were traceable from the optical trajectories obtained during the initial growth and modification. The optical properties of chromium were severely modified by the small variations in the process, which cannot be easily detectable with other characterization tools. In order to deposit metal films with consistent properties, it is very important to precisely control the deposition parameters such as pressure, power, temperature, etc. Moreover, we showed that other process-related parameters such as pumping period and air exposure were also very important factors.

Acknowledgments

The authors wish to acknowledge the financial support of KOSEF (971-0210-042-2).

References

[1] R. W. Collins and B. Y. Yang, J. Vac. Sci. Technol. B **7**, 1155 (1989)
[2] Y. -T. Kim, D. L. Allara, R. W. Collins and K. Vedam, Thin Solid Films **193/194**, 350 (1990)
[3] Y. Cong, I. An, R. W. Collins, K. Vedam, H. V. Nguyen, L. J. Pilione and R. Messier, Thin Solid Films **193/194**, 361 (1990)
[4] I. An, H. V. Nguyen, N. V. Nguyen and R. W. Collins, Phys. Rev. Lett. **65**, 2274 (1990)
[5] Y. M. Li, I. An, H. V. Nguyen, C. R. Wronski and R. W. Collins, Phys. Rev. Lett. **68**, 2814 (1992)
[6] R. W. Collins, Y. Cong, H. V. Nguyen, I. An, T. Badzian, R. Messier and K. Vedam, J. Appl. Phys. **71**, 5287 (1992)
[7] I. An and R. W. Collins, Rev. Sci. Instrum. **62**, 1904 (1991)
[8] N. V. Nguyen, B. S. Pudliner, I. An and R. W. Collins, J. Opt. Soc. Am. A. **8**, 919 (1991)
[9] I. An, Y. M. Li, H. V. Nguyen and R. W. Collins, Rev. Sci. Instrum. **63**, 3842 (1992)
[10] patent pending
[11] Y. -T. Kim and Ilsin An, Anal. Chem. **70**, 1346 (1998)
[12] D. E. Aspnes, SPIE **276**, 188 (1981)
[13] Ilsin An and Hyegeun Oh, J. Kor. Phy. Soc. **29**, 370 (1996)
[14] H. Nguyen, Ilsin An and R. W. Collins, Phys. Rev. B **47**, 3947 (1993)